



Seismic performance assessment of reinforced concrete frames strengthened using buckling-restrained braces

Birendar Karaiya¹, Dipti Ranjan Sahoo², Ashok Gupta³

¹ Ph.D. Student, Department of Civil Engineering, IIT Delhi – New Delhi, India.

² Associate Professor, Department of Civil Engineering, IIT Delhi – New Delhi, India.

³ Professor, Department of Civil Engineering, IIT Delhi – New Delhi, India.

ABSTRACT

This study presents the seismic response of low-to-high rise open ground story frames strengthened using buckling-restrained braces (BRBs). 4-story, 8-story and 20-story RC frames are considered for the seismic performance evaluation at the unstrengthened stage have been considered as the study frames. A design procedure has been proposed to determine the BRB sizes required for the target design base shear of the study frames. The seismic performance of these strengthened frames is evaluated numerically using a computer software SAP2000. The modelling technique adopted for BRBs and frame members are discussed, Linear modal analyses are carried out to determine the mode shapes and time periods of the strengthened frames. Nonlinear static and dynamic analyses are carried out to investigate the lateral strength, failure mechanism, interstory drift response and residual drift response of the study frames.

Keywords: Buckling-restrained braces; Fragility curves; RC frames; Seismic analysis; Drift response.

INTRODUCTION

The gravity load-designed (often termed as “non-ductile”) buildings with open ground story (OGS) may suffer from severely damages or complete collapse under earthquake loadings [1]. The poor seismic performance of these RC frames is primarily due to the inadequate lateral load-resistance and deformation capacity of the frame members. Some of the factors contribute to such seismic performance of a RC building primarily depends on the detailing of longitudinal reinforcing bars in frame members, the amount of confining reinforcements in columns, the amount and spacing of shear reinforcement bars in the beams, and the reinforcing detailing in the beam-column joints. Insufficient displacement ductility, rather than the inadequate lateral strength, is considered as the primary source of deficiency in the seismic performance of the gravity-load designed RC buildings [2]. Some of the existing buildings require strengthening due to the change in design guidelines, change in the occupancy type, addition of new stories to the building, or the inadequacy in material strength. Strengthening techniques are adopted to enhance the lateral strength, lateral stiffness, displacement ductility, and energy dissipation potential of the deficient structures. Recently, buckling-restrained braces are used as the lateral force-resisting systems to improve the seismic performance of the deficient structures.

Takeuchi et al. [3] presented a practical application for retrofitting an existing RC building with both BRBs and an integrated façade, increasing both the seismic and thermal performance of the building simultaneously. However, when the maximum story drift exceeds the yield point of an existing RC frame, all the structural elements, including BRBs, lose horizontal stiffness. As a result, risk of damage at a specific story and residual deformation after an earthquake is expected. Di Sarna and Manfredi [4] conducted a numerical assessment of the seismic performance of RC frame structures designed for gravity loads only and retrofitted with BRBs placed along the perimeter frames. The results of nonlinear dynamic analyses showed that more than 60% of the total energy was dissipated by the braces at the collapse-prevention limit state of frames. Cyclic tests conducted by Mahrenholtz et al. [5] on RC frames retrofitted with BRBs, directly connected through anchors, showed the enhanced lateral strength and ductility to an adequate seismic performance level. Sutcu et al. [6] proposed a seismic retrofit design method for RC buildings using BRBs and steel frames. Qu et al. [7] conducted a numerical investigation on the use of a zigzag BRB in RC buildings and concluded that the BRBs are efficient in reducing the responses of the building, even if the nonlinearity of brace connections is considered. Furthermore, strength demands for the brace connections are significantly influenced by the higher modes of the system after brace yielding.

The present study is focused on the evaluation of the seismic performance of low-to-high rise non-ductile RC frames with open ground story (OGS) strengthened using BRBs. A design procedure is proposed to determine the BRB sizes. Both nonlinear static and dynamic analyses are conducted to investigate the seismic performance of the strengthened RC frames.

DESIGN PROCEDURE

Determination of BRB sizes

The 4-story, 8-story, and 20-story OGS frames have been considered for the strengthening using BRBs in all bays in this study. It is assumed that the seismic weight of the frames would not change significantly due to the installation of BRBs only in the open stories of the study frames. Figure 1 shows the BRBs installed in the open story of a frame and the forces developed in BRBs under lateral loading. For a given value of design story shear (V_{BRB}), the tension (T) and compression (C) forces in BRBs inclined at angle of θ with horizontal can be expressed as follows:

$$V_{BRB} = (T + C) \cos \theta \quad (1)$$

The above equation is based on the assumption that the entire design story shear is resisted by BRB forces only. Design yield axial forces of BRBs in tension (P_{ty}) and compression (P_{cy}) can be determined to the material yield stress (σ_{yBRB}) and core cross-section area (A_{BRB}) as follows:

$$T = P_{ty} = \phi \sigma_{yBRB} A_{BRB} \quad (2)$$

$$C = P_{cy} = \phi \beta \sigma_{yBRB} A_{BRB} \quad (3)$$

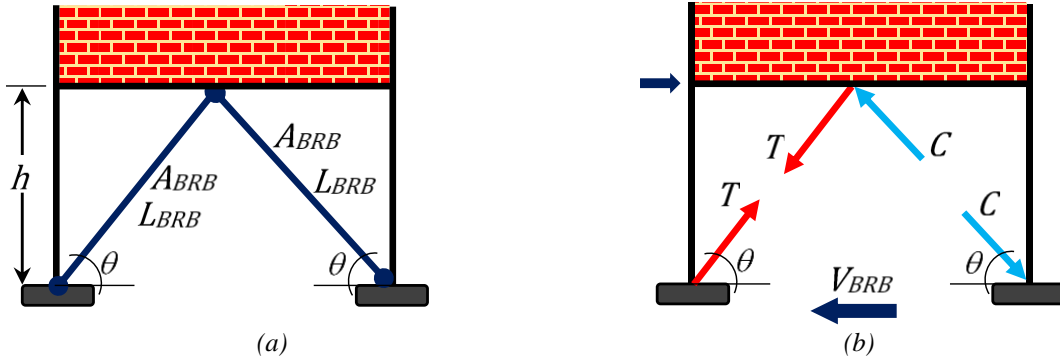


Figure 1. (a) BRBs installed in open ground story of a frame, (b) Axial forces in BRBs under the action of lateral loading

In the above equations, ϕ = strength reduction factor, which can be considered as 0.9. Figure 5.2 shows a typical BRB with different components, hysteretic response, and idealized backbone curve. The compression strength of BRB at any displacement cycle is higher than the corresponding tension strength primarily due to the Poisson's effect. The ratio of compression to tension strength of BRB at any displacement excursion is defined as compression strength adjustment factor (β). For the known values of ϕ , β and σ_{yBRB} , the required area of BRB core can be determined as follows:

$$A_{BRB} = \frac{V_{BRB}}{(1 + \beta) \phi \sigma_{yBRB} \cos \theta} \quad (4)$$

BRBs are designed in such a way that only central core segments are expected to undergo inelastic deformation, whereas both transition and end segments of BRBs, as shown in Figure 2, are designed to remain elastic. This is ensured by adopting larger cross-sections in the transition and end segments as compared to the core cross-section. The cross-section area of the transition and end segments of BRB may be taken as 1.6 and 2.2 times the area of BRB core segment. Similarly, the total length of transition segments, elastic end zones, and core segment may be taken as 6, 24, and 70% of the distance between the work points. The ultimate axial strengths of BRBs in tension and compression can be computed as the strain-hardening adjustment factor (ω) times the corresponding yield strengths. The values of β and ω for BRBs are considered as 1.10 and 1.40, respectively [9].

Computation of design base shear of strengthened frame

The dynamic behavior of an OGS frame is often considered as similar to that of the single degree-of-freedom system as the lateral displacement demand is mostly concentrated at the soft ground story level with the upper stories having masonry infill walls behaving like a rigid body. The installation of BRBs in the soft-story would contribute to the story stiffness. It is assumed that beam rotation is negligible being constrained against deformation in the presence of masonry walls under lateral loading. Therefore, the lateral stiffness (K_f) of single-story frame with columns of same height (h) and flexural rigidity (EI) can be expressed as follows:

$$K_f = \frac{24EI}{h^3} \quad (5)$$

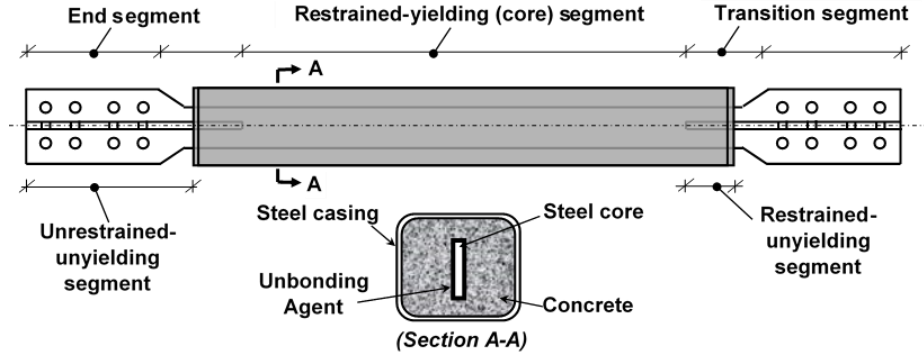


Figure 2: A typical BRB showing different segments along the longitudinal direction and cross-section

Since BRBs are connected to the beam of the portal frame, the lateral displacement would be equal assuming negligible beam deformation. Axial displacement (Δ_{BRB}) of BRBs can be related to the story sway displacement (Δ) as follows:

$$\Delta_{BRB} = \Delta \cos \theta = \frac{TL_{BRB}}{E_S A_{BRB}} \quad (6)$$

Where, E_s = Young's Modulus of BRB material (steel). Axial stiffness (K_{BRB}) of BRBs can be expressed as follows:

$$K_{BRB} = \frac{E_S A_{BRB} \sin \theta}{h} \quad (7)$$

The lateral stiffness (K'_{BRB}) contribution of BRBs can be expressed as follows:

$$K'_{BRB} = \frac{V_{BRB}}{\Delta} = \frac{T(1 + \beta) \cos \theta}{\Delta} = K_{BRB}(1 + \beta) \cos^2 \theta \quad (8)$$

Accordingly, the ratio of K'_{BRB} to K_f can be obtained as follows:

$$\frac{K'_{BRB}}{K_f} = \frac{E_S A_{BRB} h^2 (1 + \beta) \cos^2 \theta \sin \theta}{24EI} \quad (9)$$

Assuming the values of E_s/E as 8, $A_{BRB}h^2/I$ as 0.8-0.9 for a typical frame dimension and BRB sizes, θ as 45° , and β as 1.1, the ratio of K'_{BRB}/K_f can be found to be in the range 15-20%. This shows that there would not be any significant change in the fundamental period of the strengthened frame as compared to the original unstrengthened frame. Hence, it is reasonable to assume that design base shear for the strengthened frame is same as that of the unstrengthened frame.

DESIGN OF STUDY FRAMES

Three OGS frames (i.e., 4-story, 8-story, 20-story) representing low-to-high-rise structures have been considered for the strengthening using BRBs in this study. The 4-story, 8-story and 20-story OGS frames are strengthened by using BRBs in the open stories. The design base shear of 4-story, 8-story and 20-story OGS frames computed at the unstrengthened stage have been considered as the design base shear (V_{BRB}) for the strengthened frames. The design base shear values for the 4-story, 8-story and 20-story frames were computed as 428.8 kN, 465.4 kN, and 3826.5 kN, respectively. BRB core sizes are computed using the procedure discussed above and summarized in Table 1. The values of β , σ_{yBRB} , E_s are considered as 1.1, 248 MPa, 200 GPa, respectively. For computation of K_{BRB} , 70% of total BRB length has been considered in this study.

Table 1. Design area of BRB core segments in the strengthened frames

Frame	V_{BRB} (kN)	L_{BRB} (mm)	θ	T (kN)	A_{BRB} (m ²)	K_{BRB} (kN/m)
4-story	107.2	3440	54.5	77.8	0.00035	41.34
8-story	116.4	4118	60.9	84.4	0.00038	44.87
20-story	956.6	4118	60.9	694.2	0.00311	308.26

The expected axial tensile yield strengths (P_{yt}) of BRBs are computed as the product of material overstrength factor (R_y) and the nominal yield strengths (i.e., $A_{BRB}\sigma_{yBRB}$). The value of R_y is considered as 1.1. The expected axial compressive strength (P_{yc}) of BRBs is computed as the compression adjustment factor (β) times the yield strength (P_{yt}). The expected ultimate strengths (i.e., P_{ut} and P_{uc}) are computed as the tension adjustment factor (ω) times the corresponding yield strengths (i.e., P_{yt} and P_{yc}). The displacement values corresponding to tension and compression yield points are computed by dividing the yield strengths of BRBs by their axial stiffness (K_{BRB}). The computed values of expected axial resistance and displacements of BRBs in all strengthened frames are summarized in Table 2.

Table 2. Axial yield and ultimate strengths of BRBs in strengthened frames

Frame	P_{yt} (kN)	Δ_{yt} (m)	P_{yc} (kN)	Δ_{yc} (m)	P_{ut} (kN)	P_{uc} (kN)
4-story	86.4	0.0021	95.1	0.00229	121.0	133.1
8-story	93.8	0.0021	103.2	0.0023	131.3	144.5
20-story	771.3	0.0025	848.4	0.0028	1079.8	1187.8

NUMERICAL ANALYSIS

Both linear and nonlinear analyses are conducted for the strengthened frames using a computer software SAP 2000 [8]. Beams and columns of the strengthened frames are modelled as frame elements with the lumped plasticity approach adopted to represent their nonlinear force-displacement behavior. Axial force-being moment interaction as well as shear behavior is considered in the modelling of frame members. Masonry infill walls are modelled as axial three-strut elements with axial plastic hinges assigned at their mid-lengths. BRBs are connected at the mid-span of beams and column bases using pinned connections. Axial plastic hinges are assigned to BRBs at their mid-spans. The modelling parameters of BRBs are also summarized in Table 2. The post-yield stiffness of BRBs is taken as 2.5% of their elastic stiffness [9]. The strength and stiffness degradation have not been considered in the modelling of cyclic response of BRBs.

Linear Modal Analysis

Linear modal analysis is performed to investigate the time periods and mode shapes of the strengthened frames. Table 3 shows the comparison of fundamental periods and mass participation factors of un-strengthened and strengthened frames. A maximum reduction of 25% in the fundamental period is noted in the strengthened 4-story frame as compared to the unstrengthened stage. The corresponding change in the fundamental time period in 8-story frame is computed as about 15%. In case of 20-story frame, the change in fundamental period is found to be very negligible (i.e., 3%).

Table 3. Comparison of time periods of strengthened and unstrengthened frames

Sl. No	Frame	Fundamental period (sec)	
		Unstrengthened	Strengthened
1	4-story	0.35	0.28
2	8-story	0.74	0.64
3	20-story	1.12	1.09

The mode shapes of 4-story and 8-story frames showed the nearly-uniform distribution of displacement profile over the heights. The mass participation factors corresponding to the fundamental mode shapes of 4-story and 8-story frames are noted as 99.4% and 97.7%, respectively. This showed that the installation of BRBs in the soft-story levels as a strengthening measure did not

change the mode shapes of the OGS frames significantly. This is primarily due to the fact that the lateral stiffness contribution of BRBs would not be comparable to the lateral stiffness of the infill walls. The fundamental mode shape of the strengthened 20-story frame is significantly different than noted in the strengthened 4-story and 8-story frames. The mode participation factors of the 20-story frame are noted as 70.2%, 22.4%, and 5% in first three modes. This showed the higher mode contributions in the lateral displacement behavior of the strengthened 20-story frame.

Nonlinear Static Analysis

Static pushover analysis is conducted for the study frames to investigate their lateral strength, lateral stiffness, post-yield strength, and yield mechanisms. Lateral displacement profiles resembling the fundamental mode shapes of the study frames are used in the pushover analyses. The study frames are subjected to the gradually increasing lateral displacement corresponding to a roof drift of 2%. The 4-story, 8-story and 20-story OGS frames at the unstrengthened stage carried the peak lateral loads of 735.0 kN, 846.1 kN and 5368.6 kN, respectively. After strengthening, these frames carried the maximum lateral loads of 1463.2 kN, 1510.7 kN, and 6336.7 kN. A significant increase in the lateral strengths is noted in strengthened 4-story as well as 8-story frames. The increase in the lateral load carrying capacity of 4-story and 8-story strengthened frames are noted as about 100% and 80% as compared to the unstrengthened frame. However, the increase in lateral strength of the strengthened 20-story frame is noted as 15% indicating that the lateral resistance of BRBs is not fully utilized under lateral loading due to the different lateral displacement profile.

Figure 3 shows the comparison of pushover (lateral strength vs. roof drift) curves of the strengthened frames. Both 4-story and 8-story frames exhibited the improved the lateral stiffness and strength as compared to those of the unstrengthened OGS frames. The pushover curves of these frames resembled the backbone curves of force-displacement response of BRBs. The addition of BRBs resulted in the strain-hardening behavior of the strengthened frames. However, no significant improvement in the roof displacement is noted in 20-story frame. In addition, damages in ground story beams and columns are noted at the failure stage of the 20-story frame. No significant increase in the lateral stiffness is also noted in the strengthened 20-story frame. It is worth-mentioning that BRBs are designed to carry design base shear computed based on the unstrengthened OGS frames.

Figure 4 shows the comparison of hinge mechanisms of the 4-story, 8-story, and 20-story frames at the failure stage. The 4-story strengthened frame exhibited the yielding of BRBs and the yielding of columns and beams. Beams reached the collapse state under the loading at the failure stage. In case of the 8-story frame, minor yielding of the ground story columns in addition to the yielding of BRBs. No frame members reached their collapse state at 2% of the roof drift. In addition to the yielding of BRBs, damages in beams, columns and masonry infills are noted in the upper stories. As shown in the figure, beams and columns at the first story level of 4-story strengthened frame reached their ultimate stage. This showed that beams and columns of the 4-story frame are required to be strengthened in addition to BRBs in order to control the excessive damages to beams and columns. In case of the 8-story strengthened frame, plastic hinges are formed in the ground story columns as well as in the beams and columns at the second story in the exterior bays. In 20-story frame, a few BRBs in the ground story level reached their fracture stage. In addition, yielding of beams in the lower stories also noted at the hinge mechanism. The damages in masonry walls are also noted in the lower and upper stories of the 20-story strengthened frame

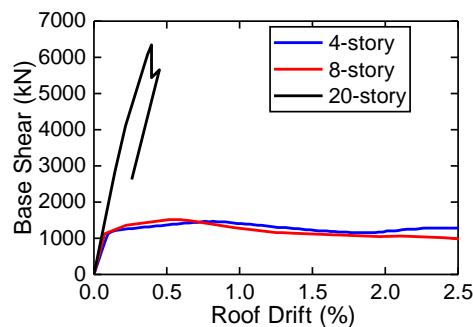


Figure 3: Comparison of capacity curves of strengthened frames

Nonlinear Time-history Analysis

Nonlinear time-history analyses are conducted for all strengthened frames using seven spectrum-compatible ground motions. Table 4 summarizes the earthquake data for the selected ground motions. These ground motions are amplitude scaled such that their mean response spectra is 10% higher than the design spectrum [10] in the period range of 0.2-1.5 times the natural periods of the structural systems. The main parameters investigated are hinge mechanisms, floor displacement response, inter-story drift response, and residual drift response. Figure 5 shows the roof displacement-time history response of 4-story strengthened

frame. The 4-story frame sustained the entire ground motions without complete collapse. No residual displacement response is noted in the 4-story frame at the end of earthquake load application. The 8-story frame exhibited the significant residual displacement at the end of load applications. This is clearly observed in the hinge mechanism of the 8-story frame where the plastic hinges in columns and beams at the first story level reached their ultimate states. The 20-story frame survived the entire duration of earthquake excitations of all selected ground motions. Unlike the 8-story frame, the 20-story frame did not exhibit the residual displacements at the end of loading.

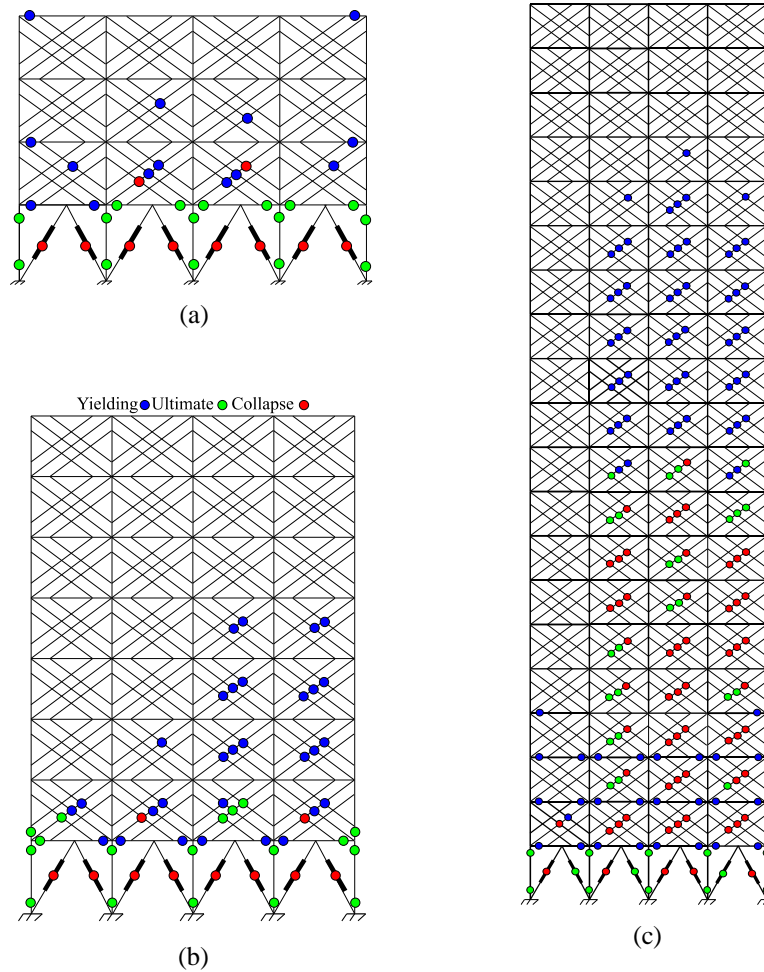


Figure 4. Comparison of hinge mechanism of strengthened frames (a) 4-story, (b) 8-story, (c) 20-story

Table 4. Earthquake data and site information of the selected ground motions

Sl. No	Earthquake name	Station	Magnitude (M_w)	Distance (km)	PGA (g)	Total time (sec)
1	Northridge Earthquake (1994)	Canyon Country, WLC	6.7	26.5	0.41	20.00
2	Hector Mine Earthquake (1999)	Hector	7.1	26.5	0.27	45.32
3	Kobe (Japan) Earthquake (1995)	Shin-Osaka	6.9	46	0.24	41.00
4	Kocaeli (Turkey) Earthquake (1999)	Arcelik	7.5	53.7	0.15	30.00
5	Superstition Hills Earthquake (1987)	Poe Road (temp)	6.5	11.2	0.45	22.30
6	Cape Mendocino Earthquake (1992)	Rio Dell Overpass	7.0	22.7	0.24	56.02
7	Chi-Chi (Taiwan) Earthquake (1999)	TCU045	7.6	77.5	0.40	90.00

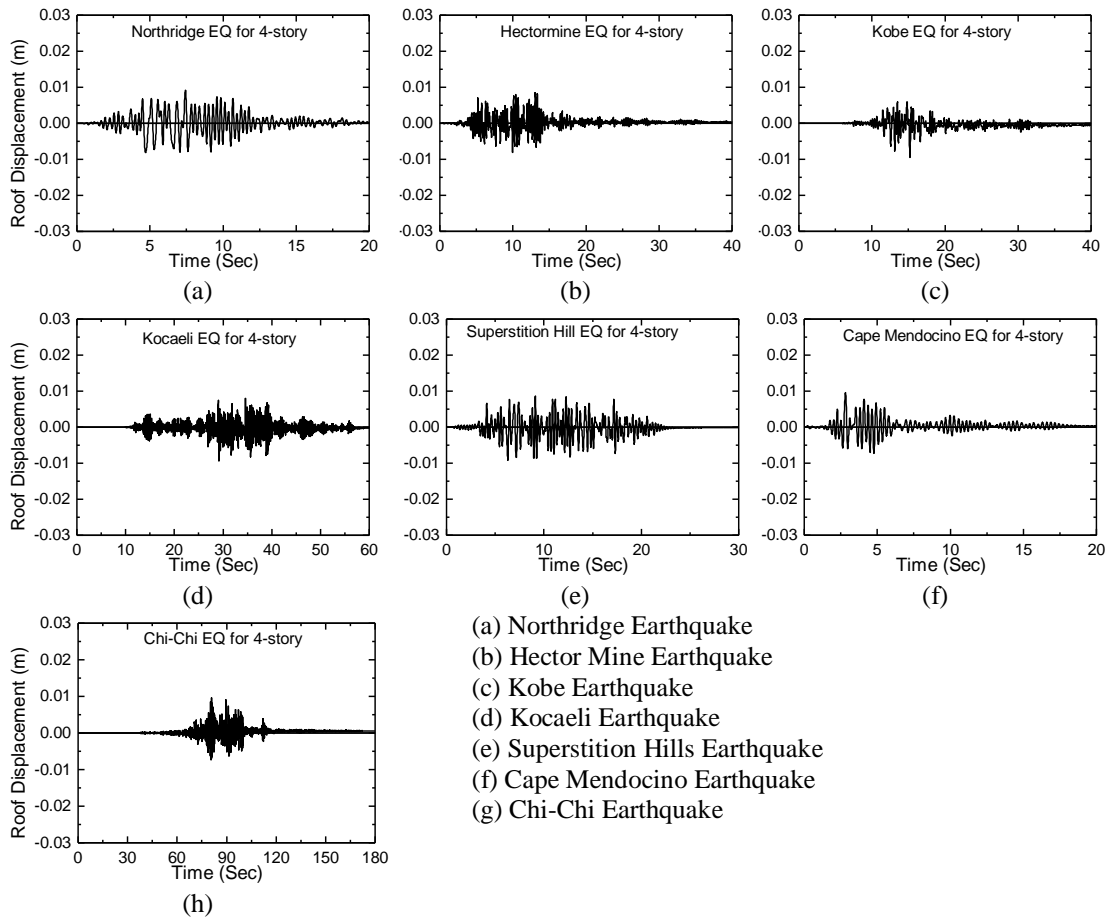


Figure 5. Roof displacements vs. time response of the 4-story frame

Figure 6 shows the comparison of inter-story drift ratio (ISDR) response of all strengthened frames. The peak value of average ISDR response of 4-story frame is noted as 0.34%, the corresponding values for the 8-story and 20-story are observed as 1.45% and 0.27%. The peak ISDR response is noted at the first story of the 4-story and 8-story frames. The average values of ISDR noted in the remaining stories are very small in the magnitude as compared to those observed at the first story level. The distribution of average ISDR response of the 20-story frame is fairly uniform over the height. The peak values of ISDR response are gradually increased over the height of the frame. Further, the peak values of ISDR response noted in the 20-story frame are significantly smaller than those noted in the 4-story and 8-story strengthened frames. In contrast to the 4-story and 8-story frames where the peak ISDR values are noted at the first story level, the 20-story frame exhibited the peak values of ISDR response in the upper stories (i.e., in the 14th to 16th stories).

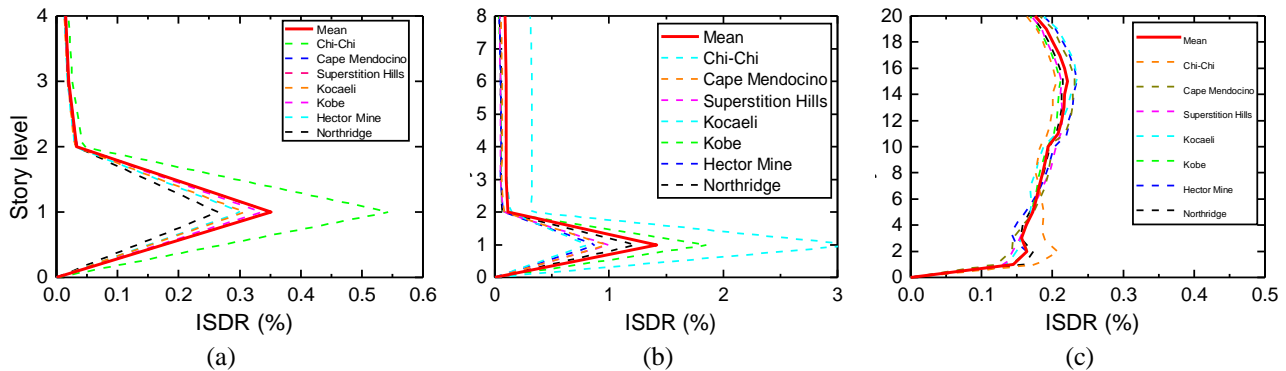


Figure 6. Comparison of inter-story drift response of strengthened OGS frames (a) 4-story, (b) 8-story and (c) 20-story

Figure 7 shows the comparison of residual drift response (RDR) of the strengthened frames. The distribution of average peak RDR response over the height of the frames is similar to that of the ISDR response. The peak value of average RDR response of the 4-story frame is found to be very negligible. The maximum value of peak RDR response is noted at 0.51% at the first story of the 8-story strengthened frame. Similarly, the 20-story frame exhibited the negligible average peak RDR response. The same RDR response can be inferred from the roof displacement-time response as discussed earlier. The peak RDR response is uniformly distributed over the height of the 20-story frame.

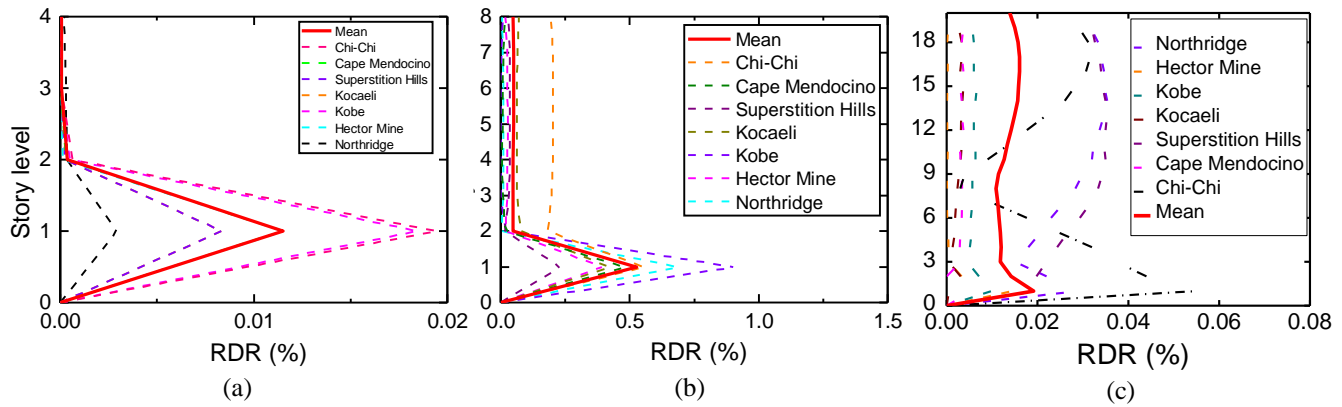


Figure 7. Comparison of residual drift response (RDR) of strengthened frames (a) 4-story, (b) 8-story, (c) 20-story

CONCLUSIONS

The following conclusions can be drawn as follows:

- The installation of BRBs in the ground story reduced the fundamental time period of 4-story and 8-story structures by 15–20%. No significant reduction in the time period of 20-story frame due to the installation of BRBs in the ground story only.
- The design of BRBs for a target base shear equal to the that of the OGS frame successfully helped the strengthened frame to sustain the entire duration of the selected ground motions without premature failure as observed in the former case.
- Beams and columns of the 4-story and 8-story strengthened frames reached their yielding limits without attaining their collapse states under seismic loading. BRBs resisted the nearly the entire lateral loads which reduced the demand on the ground story columns and beams.
- BRBs in the 20-story frames did not yield under the selected ground motions, whereas the beams and column showed the minor yielding. This showed that BRBs are not cost-effective strengthening elements in the high-rise OGS frames.
- Further investigation is required to generalize the conclusions presented in this

REFERENCES

- [1] Jain SK, Lettis WR, Murty CVR, Bardet JP. *Bhuj, India, Earthquake of January 26, 2001*, Reconnaissance report, 2002.
- [2] Priestley MJN. Displacement-based seismic assessment of reinforced concrete buildings. *Journal of Earthquake Engineering* 1997; **1**(1): 157–192.
- [3] Takeuchi T, Yasuda K, Iwata M. Studies on integrated building facade engineering with high-performance structural elements. *IABSE Symposium Report*, 33–40, 2006.
- [4] Di Sarno L, Manfredi G. Seismic retrofitting with buckling restrained braces: Application to an existing non-ductile RC framed building. *Soil Dynamics and Earthquake Engineering* 2010; **30**(11): 1279–1297.
- [5] Mahrenholtz C, Lin PC, Wu AC, Tsai KC, Hwang SJ, Lin RY, Bhayusukma MY. Retrofit of reinforced concrete frames with buckling-restrained braces. *Earthquake Engineering and Structural Dynamics* 2015; **44**(1): 59–78..
- [6] Sutcu F, Takeuchi T, Matsui R. Seismic retrofit design method for RC buildings using buckling-restrained braces and steel frames. *Journal of Constructional Steel Research* 2014; **101**, 304–313.
- [7] Qu Z, Kishiki S, Maida Y, Sakata H, Wada A. Seismic responses of reinforced concrete frames with buckling restrained braces in zigzag configuration. *Engineering Structures* 2015; **105**: 12–21.
- [8] CSI. *Structural Software for Analysis and Design | SAP2000*, Computers and Structures, Inc, Berkeley, USA, 2016.
- [9] Sahoo DR, Chao S-H. “Performance-based plastic design method for buckling-restrained braced frames.” *Engineering Structures* 2010, **32**(9), 2950–2958.
- [10] IS:1893 (Part 1). *Criteria for earthquake resistant design of structures*. Bureau of Indian Standards, New Delhi, India, 2016.